BE FLOOD READY

Remote Sensing in Flood Monitoring

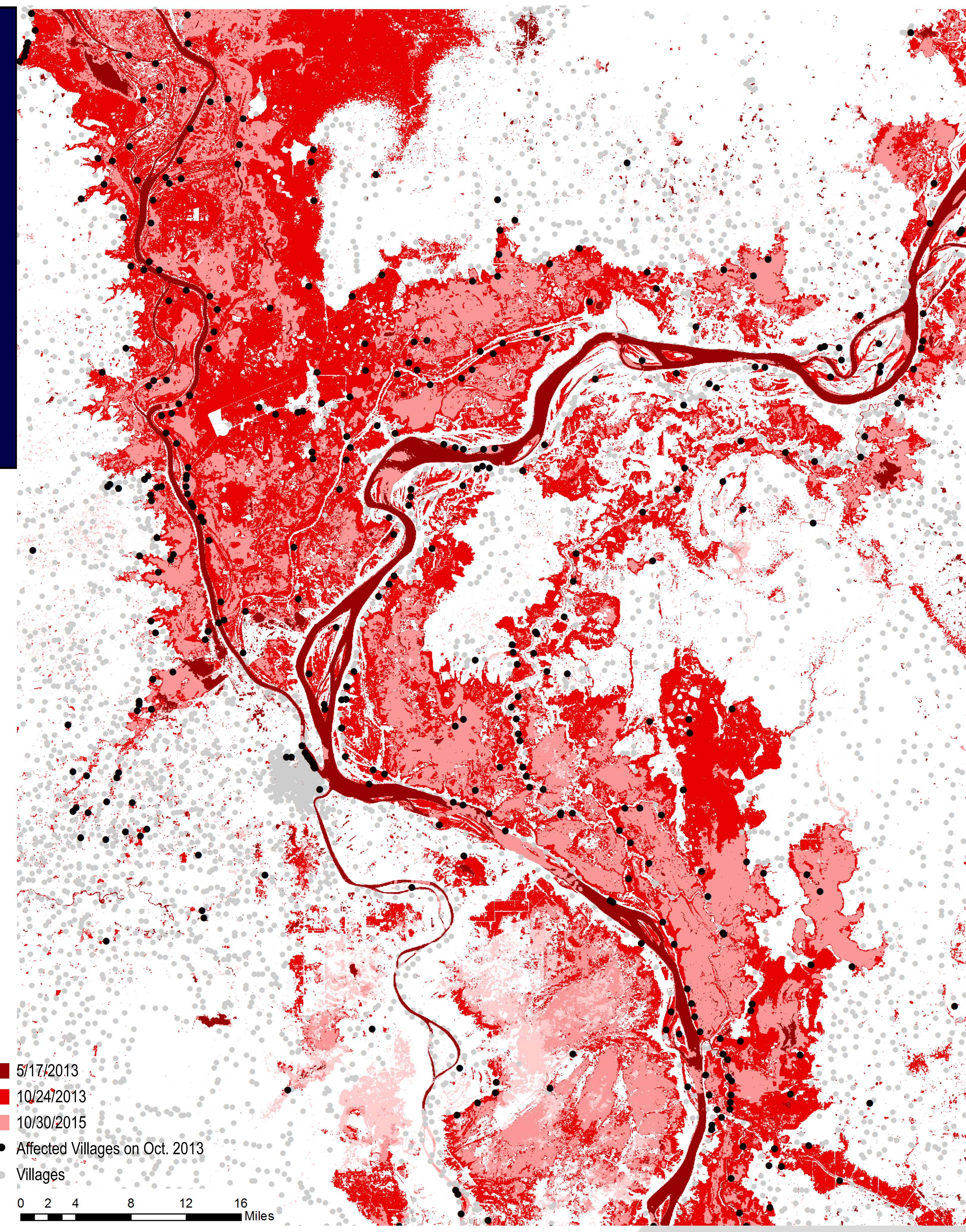

THE WATER BODIES IN DIFFERENT TIME SERIES AND THE DEMOGRAPHICS

INTRODUCTION

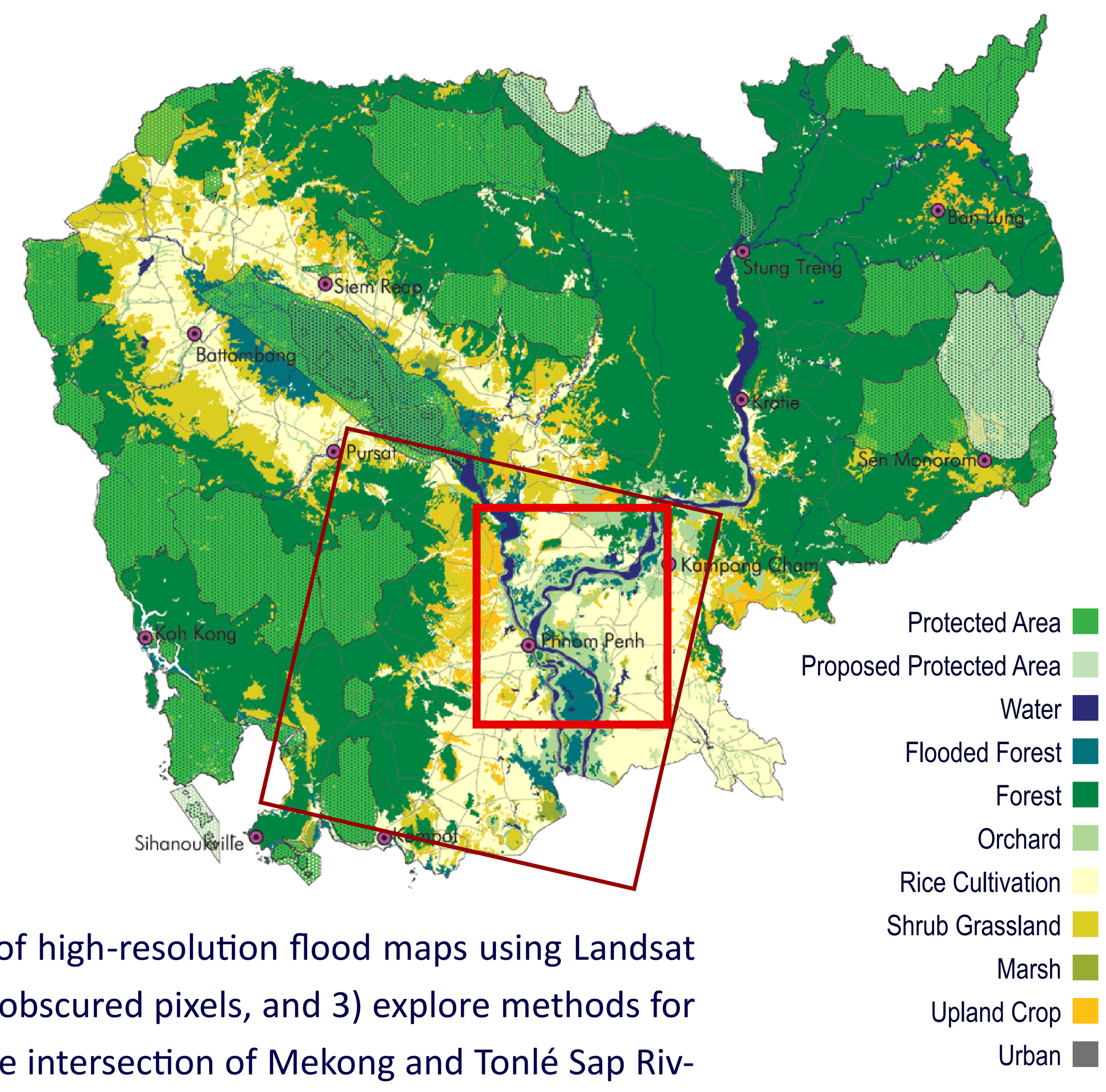

In October 2013, Typhoon Nari followed heavy seasonal rains creating substantial flooding along the Mekong and Tonlé Sap Rivers in Cambodia. The flood affected half million lives, destroyed about three-quarters of a million acres and caused huge economic loses. Precise knowledge of inundated areas is essential when it comes to putting immediate relief efforts, detecting deficiencies and planning future mitigation in terms of flood control mechanisms. The use of remote sensing provides tremendous potential for identification, monitoring and assessment of flood disaster.

The objective of this study is to 1) generate a series of high-resolution flood maps using Landsat 8 images, 2) evaluate the performance of masking cloud-obscured pixels, and 3) explore methods for flood detection. The October 2013 flood event around the intersection of Mekong and Tonlé Sap River, Cambodia is used as a case study. The landscape of the study area is characterized by a low-lying plain, with a wide variety of land cover types. Like the rest of Southeast Asia, Cambodia experiences tropical monsoons, known as wet and dry seasons. Southwest monsoons blow inland bring moisture-laden winds from Indian Ocean from June to November. Northeast monsoons last which results in dry period from December to May. Hence, a time series of images between dry and wet seasons are necessary to identify the agents of change during the flood event.

Three Landsat 8 images downloaded from USGS Earth Explorer were processed to identify flooded areas affected by Typhoon Nari (RGB: Blue, NIR, SWIR; Linear2%). The choice of this specific period was due to the monsoon mentioned above, and availability of the 16-day overpass cycle of the Landsat 8 with limited cloud cover. The images acquired on May 17, 2013 (TIME1) and October 30, 2015 (TIME3) were used for pre-flood analysis in dry season and wet season, respectively. For the during-flood image, the Landsat 8 image captured on October 24, 2013 (TIME2). I then resized the three images in order to exclude some of the clouds and make the study area more precisely.

TIME1: 5/17/13 DRY SEASON

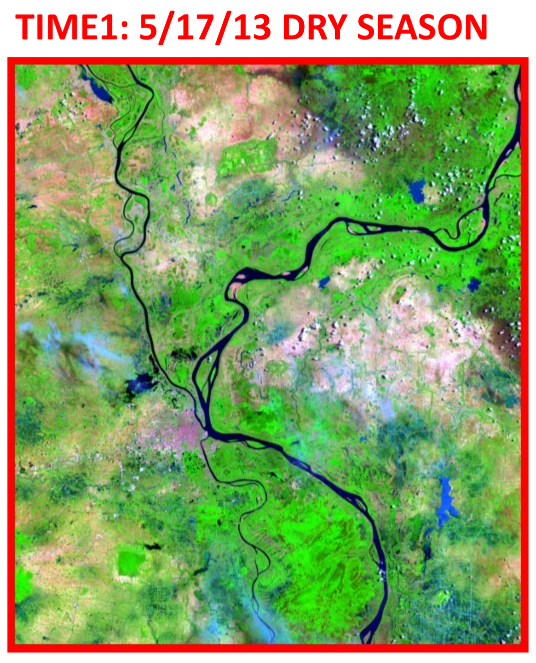

TIME2: 10/24/13 FLOODED

TIME3: 10/30/15 WET SEASON

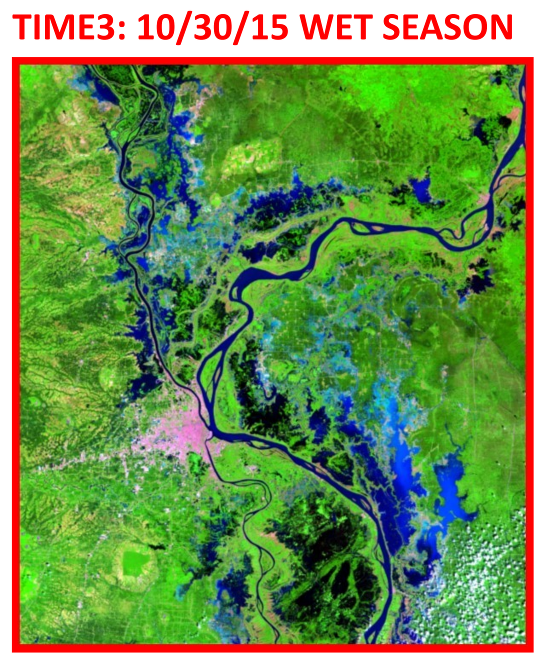

METHODOLOGY

To quantify the flood area, a series of masks were created in ENVI. First, the water bodies mask was created from observing the water pixels in Near Infrared (NIR) Band. Pixels range below 11,000 excluded other information, and well extracted water data. Then I created a Region of Interest (ROI) by applying the BQA images to build up a cloud mask. Landsat 8 Level-1 data products include a 16-bit Quality Assessment Band file (BQA.tif) representing bit-packed combinations of surface, atmosphere, and sensor conditions that can affect the overall usefulness of a given pixel. In the ROI tool dialog, I selected all possible thresholds for cloud and cloud shadow. The three maps were compared through change detection analysis to quality land cover and flooded area changes. After applying cloud mask and water mask, I conducted change detection using band algebra: (float(b1)-float(b2)). Then I add color slices and limited the unchanged pixel values from -1222 to 1222. Afterwards, I transformed the water bodies into shapefiles in ArcMap.

TIME1 v. TIME3 DETECTED CHANGES

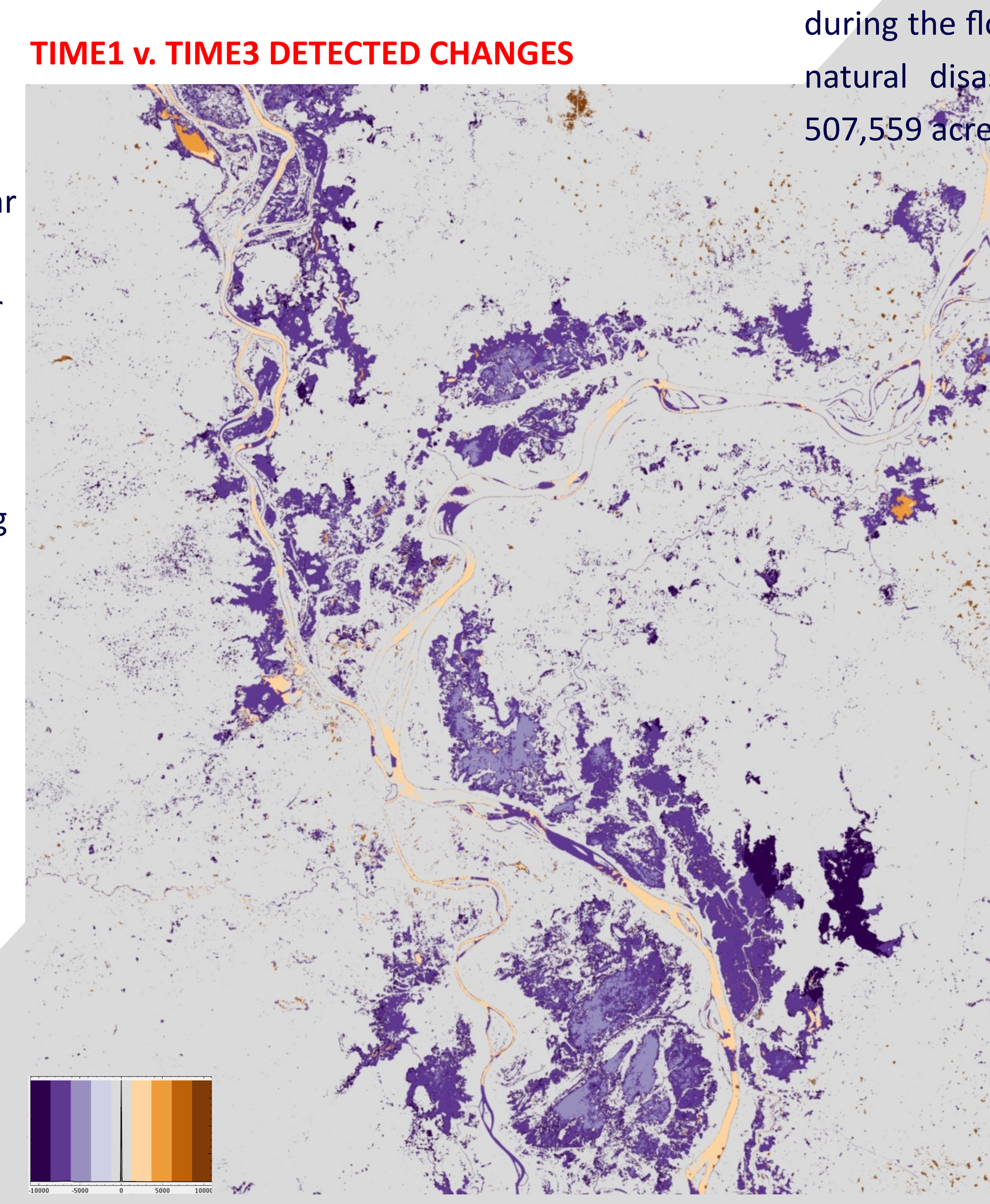

RESULTS

The multi-season analysis were conducted to detect the changes of water bodies between monsoons. In IMG7, negative pixels represented areas suffering routing floods. The dark purple provided area with highest negative pixel values which helped to identify the greatest seasonal water changes. Pixels from -1222 to 1222 was identified as unchanged area (shown in gray). In general, the permanent water bodies should be characterized as unchanged area. However, the result indicated slightly changes (light-yellow area) along the riverbed. This is because of the difference between the depth of river during monsoon.

The flood maps were presented in IMG8. The flood areas were characterized by subtracting the waters in prior dry season in the same year and in general wet season (same month but different year). The negative pixels (red) represented the flood area. On the other hand, the positive pixels (green or blue) indicated areas in the lower left corner of the Time2 image was affected by haze.

In the dry season of May 2013, the Mekong and Tonlé Sap Rivers was 98,026 acres, representing the permanent water bodies in dark red. Between May and October 2013, water increased by 918,677 acres, in particularly affecting 382 villages and 444,765 population during the flood period. In comparison with same season without any natural disasters at 30th October 2015, Typhoon Nari produced 507,559 acres of water bodies.

CONCLUSION

In this paper, the 2013 extreme flood event and the water bodies during monsoon season in Phnom Penh, Cambodia were analyzed. The study was performed by processing three Landsat multispectral and QBA images. To quantify the flood area, I applied masking and change detection method in ENVI. A series of masking approach for estimating flooding in pixels obscured by clouds were presented. This was used successfully to exclude clouds and identify flood water pixels. The approach clarified the number of water pixels available for change detection and, in turn, improved the fitness with the reference images. Band Math using for change detection yielded high accuracy to compare water bodies in different images.

Future research will include the development of a topography-based approach for identifying flood water pixels beneath clouds. Another attempt is to point out water pixels beneath the vegetation canopy in order to improve the accuracy of flood detection. It is also envisioned to apply the cloud cover correction technique and the flood water change detection algorithms to expedite this process.

TIME1 v. TIME2 DETECTED CHANGES

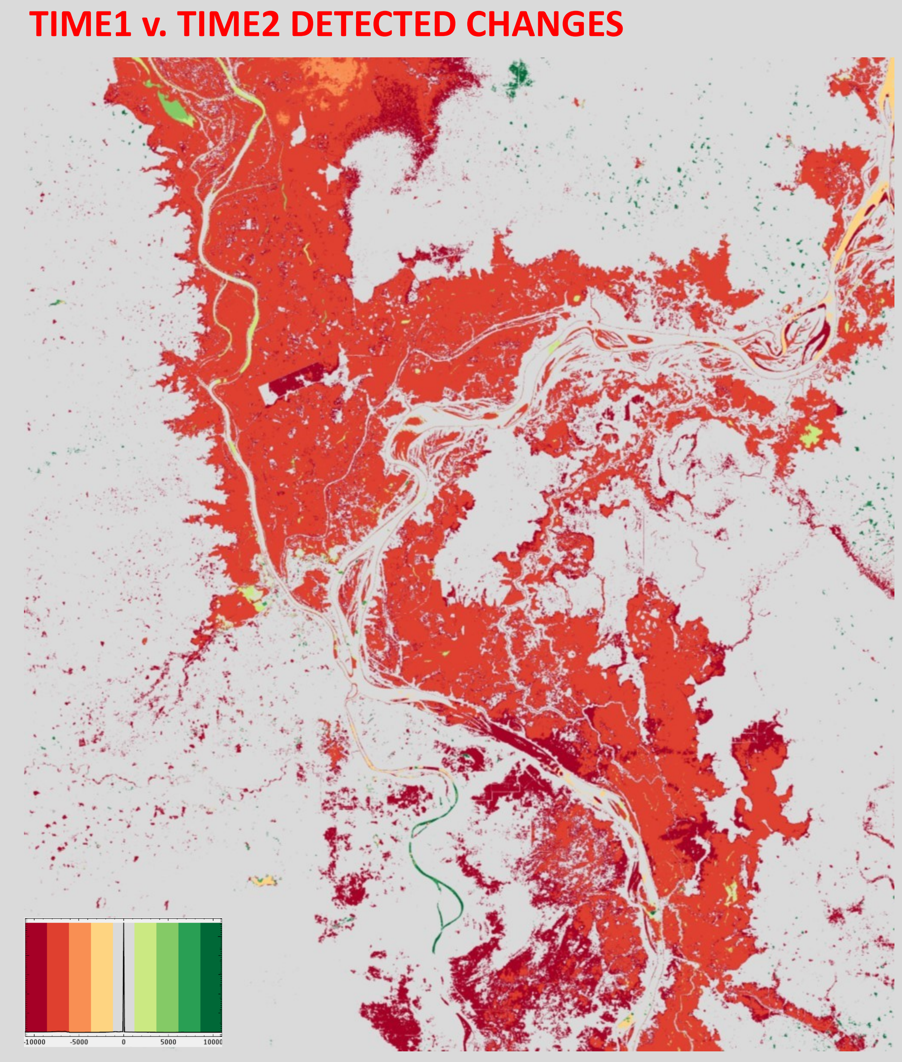

TIME3 v. TIME2 DETECTED CHANGES

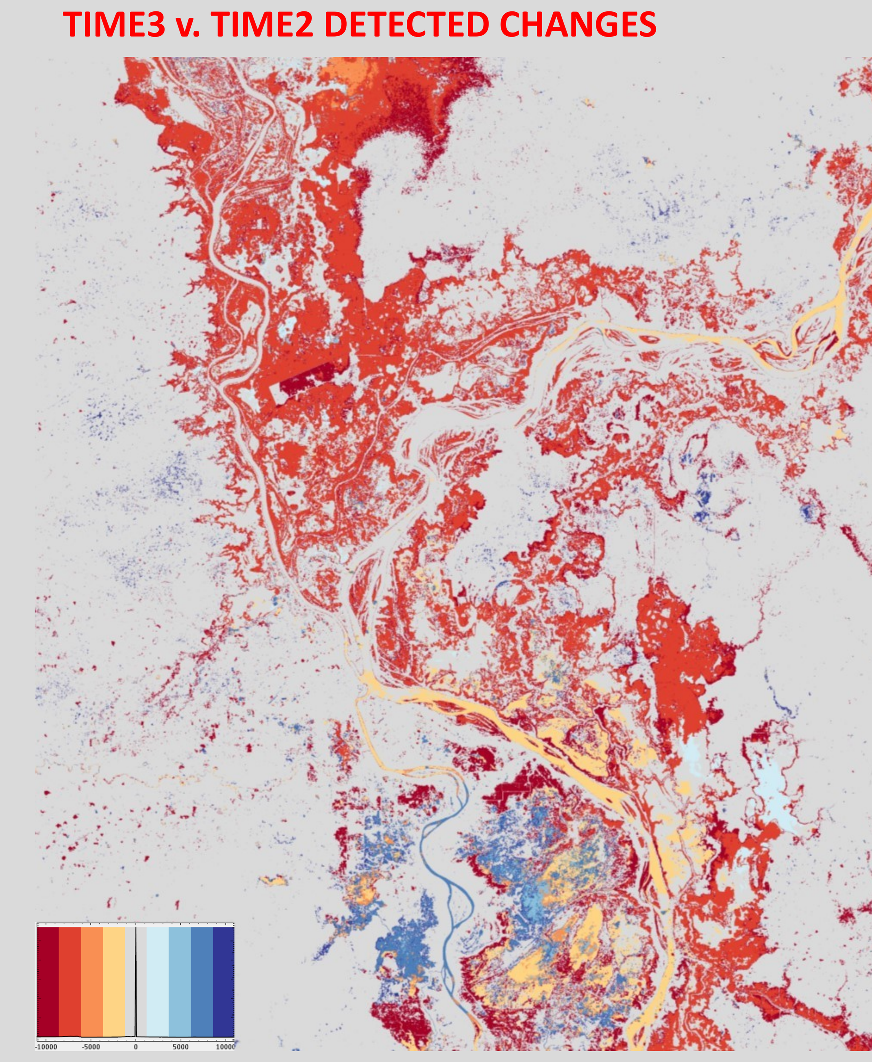

Tufts UNIVERSITY

JU YING HUNG | MAY 2018 | CEE189

Urban & Environmental Policy & Planning

Data Sources: USGS, M Drive, ICEM

Projection: WGS 1984 UTM Zone 48N